Cascaded Micro Wind Turbine Braking Mechanism via Dynamic Braking and Yaw Control

Muhammad Zulfadli Zolkifly , Norkharziana Mohd Nayan , Ami Nurul Nazifah Abdullah, Siti Khodijah Mazalan, Zainuddin Mat Isa, Mohd Hafiz Arshad
Power Electronics Control and Optimization Research, Group (PECO),
Center of Excellence for Renewable Energy (CERE),
School of Electrical System Engineering, Universiti Malaysia Perlis (UniMAP).
norkharziana@unimap.edu.my

***Abstract*—This work proposes a cascaded braking mechanism. It consists of dynamic braking and yaw control scheme. Both schemes provide safety of the micro-wind turbine operation. It protects from over speed and also functioning as speed regulator. The goal of this study is to extend the lifespan of micro wind turbine by preventing it from over speed condition. The Proportional Integral Derivatives (PID) algorithm is used to control the braking mechanism based on Integral Time Absolute Error (ITAE) criteria to determine its coefficient. The proposed mechanism able to maintain rotational speed under the maximum limit when wind speed increase from 4.8-5.2 m/s without the needs to shutdown operation.**

***Index Terms*—PID Control; Multi Rotor Configuration; Micro Wind Turbine; Braking Mechanism**

I. INTRODUCTION

Multi-rotor configuration is developed to overcome the difficulties of producing a large blade with a specific characteristic such as low mass with high strength capabilities due to lack of advanced technology. These requirements involve with upscaling theory when power generation scales with the size of the blade. The upscaling theory has a limitation because the mass of wind turbine increased in cubic, while the power generated an increase in the square. The idea of installing multiple rotor small wind turbine is to boost power generation that equivalent to the single unit large wind turbine [1]. Therefore, due to smaller blade size and the generator, the mass was significantly reduced. For a micro wind turbine, its output power is less compared with small scale wind turbine [2]. Due to its low power generation, its application can be focused on standalone power applications such as charging battery and outdoor applications [3].

Micro wind turbine is expected to harvest maximum wind power from the low range of wind speed. In terms power generation perspective, high wind speed is significant as it can produce more electrical power and support more loads. However, when micro wind turbine operated at high wind speed region, it has a major drawback such as shorten its bearing life span and increase the possibility for support structure failure due to the high impact of vibration. For multi-rotor configuration, the swept area of wind turbine also increased. During gust wind, the wind speed can rise up to 7.71 m/s and above in a short duration. This may cause one of wind turbine experiences different wind flow from one another. As a result, these cause one of wind turbine rotors to accelerate extremely which may lead to over speed condition. This condition requires control mechanism to regulate each of rotor speed at safe operating level when wind speed suddenly exceed rated speed.

II. LITERATURE REVIEW

There are two main elements involve in the braking mechanism such as the mechanical and electrical component that used in braking and another element is control theory for the braking systems. From the literature search, there were few types of an existing mechanism such as yaw mechanism, furling mechanism, and dynamic braking. Yaw system is a mechanism that rotates nacelle along the horizontal axis for a horizontal wind turbine. This system can be categorized as passive yaw and active yaw system. Passive yaw system is a system that depends on the alignment of wind directions. This system eliminates the need for a motor for alignment of the wind turbine to the wind direction. However, this system only useful for light weight or a small wind turbine. The disadvantage of this system, when the sudden gusty wind blows, the system follows direction high wind speed which can damage the wind turbine. An active yaw system has an advantage over passive yaw system where it has an anemometer attached to provide feedback element to the controller. It ensures that the system applies the brake when the wind speeds over a threshold value. Study of active yaw system in [4] demonstrated the used of worm gear mechanism to provide rotation along the vertical axis for speed reduction and high torque capabilities for yaw motor. Figure 1 shows the operation of wind turbine changes it orientation when subjected to the wind direction (W1 and W2) changes.

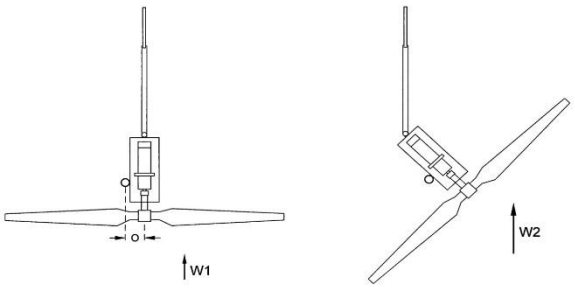

Figure 1: Yawed wind turbine

The furling mechanism is similar to the passive yaw mechanism, but it main purposes for over speed protection. The mechanism inside the furling system has hinged on the main body of a wind turbine. It was designed to have offset angle between tail fin to keep it balance during normal

operation. The principle of furling mechanism involves with thrust force acting on the blade of the wind turbine. During high wind speed, the total thrust force acting blade of wind turbine allows it turn around either horizontal or vertical axis for speed protection purpose [5].

Figure 2: Furling mechanism
(Photo courtesy of NREL - Dean Davis.)

Dynamic braking is a method of small wind turbine control that involves short-circuiting the generator stator windings. This short-circuit results in a large back-torque whose magnitude depends on rotation speed and configuration of the generator; two principal configurations are radial or axial flux designs [6]. The acceleration of the wind turbine rotor depends on the net torque namely a net positive torque which will cause the rotor to accelerate and a net negative torque that will result in deceleration. For high wind speeds condition; the magnitude of the rotor torque exceeding back-torque frequently. In certain circumstance, it is impossible for dynamic braking to make wind turbine decelerate. Although, dynamic braking has a disadvantage which it cannot force wind turbine to stop, the rotational speed can be reduced without involving mechanical brake. This is an advantage for micro wind turbine because the installed mechanical brake was not a feasible solution. The dynamic series resistor configuration was proposed for over current protection that was described in [7]. However, to limit the rotational speed of rotor the dynamic resistor involve with DC generator must be in parallel connection.

In the aspect of control theory for a braking mechanism, there several methods that had been review such as maximum power point (MPPT), sliding mode control (SMC) and Proportional Integral Derivatives (PID) control. The maximum point power tracking (MPPT) is an algorithm that widely uses in the solar panel where the maximum power is extracted. This concept also can be applied to the wind turbine where the maximum power from wind extracted when wind direction perfectly with an aligning of the wind turbine. Although in real condition, yaw misalignment still exists in a small range of error. This concept was mention by A. Mesemanolis in their research associated with yaw control in the alignment of wind direction with the nacelle [8]. However, different with the braking application, assume the previous power generation is maximized, adjustment yaw angle considers as yaw misalignment.

Sliding mode control (SMC) is a robust control system that seeks error convergence to the zero by utilized error tracking as mean of control. This technique was popular due to simplicity in design control system. In terms of wind turbine application, the aerodynamic of a wind turbine does not need to be modeled as mention by Yun She [9] in her research. The aerodynamic torque acting on wind turbine was considered as disturbance thus eliminate the need for wind speed measurement. Nevertheless, it can produce chattering phenomena where high-frequency switching become a problem when controlling mechanical actuator. Thus, a super twisting algorithm was used by [10] by eliminating chattering phenomena. Without derivative's term in error tracking, the high gain in controller setting makes system oscillate around the set point.

III. Research Methodology

A. Modeling of output winds power

The mathematical model of yawed micro wind turbine can be modeled by wind power equation as in equation 1 referred to [11]. This mathematical equation shows the power extracted from micro wind turbine when yawed condition. The increased in offset angle between wind turbine with the direction of the wind, reduce the power extract thus reducing aerodynamic torque

$$P = \frac{1}{2}\rho A V^3 C_P \cos\theta \quad (1)$$

$$T = \frac{1}{2}\rho A r^3 V^2 C_t \cos\theta \quad (2)$$

where: P = power extracted by wind turbine
T = aerodynamic torque produced
ρ = air density which is 1.22 kg/m^3
C_t = coefficient of torque for wind turbine
C_p = coefficient of power (limits to 0.53 according to Benz law)
A = swept area of blade when rotating
V = average incoming wind speed enter wind turbine
θ = yaw angle which respect to direction of wind flow
r = radius of blade.

The relationship between aerodynamic torque and angular speed of wind turbine is described by using Newton second law of motion as in Equation 3. Equation 3 shows that if positive net torque applied to the wind turbine, the wind turbine will accelerate. In meanwhile, if net torque is negative, it shows that wind turbine will experience a deceleration.

$$\beta\omega + J\alpha = T_a - T_g \quad (3)$$

where: B = viscosity of friction
J = momentum of inertia
α = angular acceleration
T_a = aerodynamic torque
T_g = generator torque
ω = angular speed in rad/s

B. Linearization of wind turbine

The graph in Figure 3 shows relationships coefficient of torque is a hyperbolic function with respect to tip speed ratio, λ (TSR). In linear control, Equation 2 is linearized at the certain operating point. Taylor expansion series is used by assuming the change in aerodynamic torque and angular speed is small, given Equation 4.

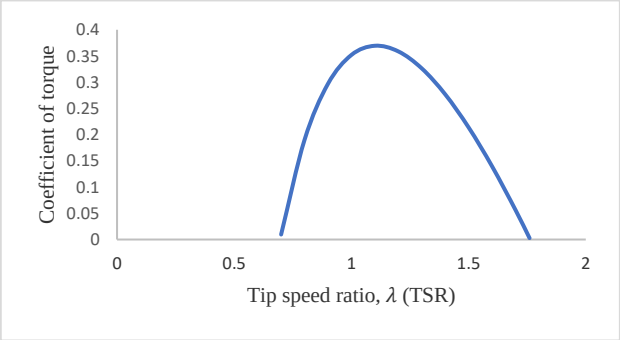

Figure 3: Coefficient of torque of micro wind turbine

$$\Delta T_a = \delta \Delta V + \gamma \Delta \omega \tag{4}$$

$$\lambda = \frac{\omega R}{V} \tag{5}$$

where λ = tip speed ratio.

$$\frac{d\Delta\omega(t)}{dt} = \frac{1}{J}\left(\Delta T_g + \Delta V\delta + \gamma\Delta\omega - \beta\Delta\omega\right) \tag{6}$$

From Equation 6, the transfer function of wind turbine that relates to the angular rotation is depicted in Equation 7. Equation 10 shows the transfer function of the system is in first order model with no zero. The block diagram for the wind turbine can be seen in Figure 4.

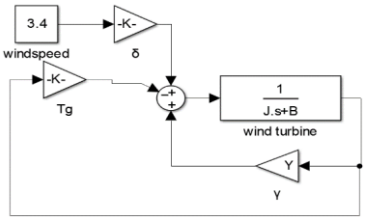

Figure 4: Block diagram of wind turbine

$$\frac{\omega}{T_g} = \frac{1}{Js + \beta - \gamma} \tag{7}$$

$$c(s) = Js + \beta - \gamma \tag{8}$$

$$s = -\frac{\beta}{J} + \frac{\gamma}{J} \tag{9}$$

The characteristic equation in 11 shows that poles in the systems depend on γ. The location of poles which can be located on right-hand side in S plane if γ is more positive than β. By knowing the poles location, the controller can be designed to compensate the effect of γ to ensure the stability of the system. If the γ outside from linearized model, the system is no longer operated in linear mode this is because certain parameter was not modelled or inaccurate model of the system.

C. Modelling DC generator

The generator torque is modeled to get the transfer function between torque rotor developed by the induced current. By substituting the Equation 10 and 11 into Equation 12, it yields Equation 13.

$$E = k_\emptyset \omega \tag{10}$$

$$I = \frac{k_\emptyset \omega}{R} \tag{11}$$

$$T_g = k_\emptyset I \tag{12}$$

$$T_g = \frac{k_\emptyset^2 \omega}{R} \tag{13}$$

where: ω = angular speed, in rad/s
$k_\emptyset$ = Back electromagnetic force constant of the DC generator
E = Induced voltage of DC machine
T_g = Torque generated by generator
I = Current flow out terminal
R = Total resistance of DC generator

D. Modelling DC motor

The yaw actuator consists of the DC motor which allows yaw angle to be controlled. The Figure 5 shows, that the schematic diagram of the DC motor that is used to develop the differential equation with respect to angle.

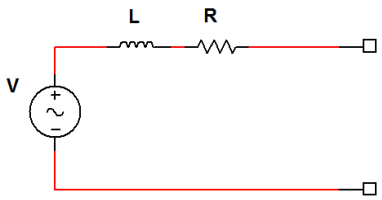

Figure 5: Schematic of DC motor

By substitute Equation 14 till 16 into 17 gives Equation 18,

$$V = iR + E \tag{14}$$

$$E = k_\emptyset \omega \tag{15}$$

$$T_d = k_\emptyset i \tag{16}$$

$$B\omega + J\frac{d\omega}{dt} = T_d \tag{17}$$

$$B\frac{d\theta}{dt} + J\frac{d^2\theta}{dt^2} = k_\emptyset \frac{\left(V - k_\emptyset \frac{d\theta}{dt}\right)}{R} \tag{18}$$

$$\frac{\theta(s)}{V(s)} = \frac{k_\emptyset}{(Js^2 + Bs)R + k_\emptyset^2 s} \tag{19}$$

Simplifying equation 18 yields transfer function Equation 19 show that angle increased when voltage input is given into the system.

E. PID Tuning via ITAE

The PID is tuned base on the ITAE criteria started by finding initial coefficient for k_d, k_p and k_i. This tuning gives the lower overshoot and faster settling time. However, tuning also had limitation since the output from the controller cannot exceed maximum input for dynamic braking resistor. Besides that, this braking system involves with single input multiple outputs (SIMO) which need two controllers that control their own actuator. This involves a detuned process to differentiate between actuators operation. Base on Table 1, the controller is tuned by criterion given, which depends on the order of close-loop transfer function.

Table 1
ITAE criteria for step input

Order	Optimum coefficient
1	$s+\omega_n$
2	$s^2+1.4\omega_n s+{\omega_n}^2$
3	$s^3+1.75\omega_n s^2+2.15{\omega_n}^2 s+{\omega_n}^3$
4	$s^4+2.1\omega_n s^3+3.4{\omega_n}^2 s^2+2.7{\omega_n}^3 s+{\omega_n}^4$
5	$s^5+2.8\omega_n s^4+5.0{\omega_n}^2 s^3+5.5{\omega_n}^3 s^2+3.4{\omega_n}^4 s+{\omega_n}^5$
6	$s^6+3.25\omega_n s^5+6.6{\omega_n}^2 s^4+8.6{\omega_n}^3 s^3+7.45{\omega_n}^4 s^2+3.95{\omega_n}^5 s+{\omega_n}^6$

The transfer function of dynamic braking with controller shown in Equation 20.

$$T(s)=\frac{\left(k_d s^2+k_p s+k_i\right)k\phi}{JRs^2+BRs-\gamma Rs} \tag{20}$$

Characteristic equation for system become Equation 22.

$$T(s)=\frac{G(s)}{1+G(s)H(s)} \tag{21}$$

$$T(s)=JRs^2+BRs-\gamma Rs+\left(k_d s^2+k_p s+k_i\right)k\phi \tag{22}$$

$$T(s)=s^2\left(JR+k\phi k_d\right)+s\left(BR-\gamma R+k_p k\phi\right)+k_i k\phi \tag{23}$$

By comparing Equation 22 and 23 with the criterion, gives coefficient in term of proportional, integral and derivatives, denoted by k_p, k_i, and k_d as can be seen in Equation 24 to 26.

$$k_p=\frac{1.4\omega_n-BR+\gamma R}{k\phi} \tag{24}$$

$$k_i=\frac{\omega_n^2}{k\phi} \tag{25}$$

$$k_d=\frac{1-JR}{k\phi} \tag{26}$$

For yaw control by using ITAE tuning, the plant with the controller transfer function becomes Equation 27.

$$\frac{k\phi(k_d s^2+k_p s+k_i)}{(Js^3+Bs^2)R+k\phi^2 s^2} \tag{27}$$

From the Equation 27, the characteristic equation can be formed by using close-loop transfer function as in Equation 28.

$$C(s)=s^3+s^2\left(\frac{B}{JR}+\frac{k_\phi^2}{JR}+\frac{k_\phi k_d}{JR}\right)+s\left(\frac{k_p}{JR}\right)+\frac{k_i}{JR} \tag{28}$$

By comparing criterion in Table 3 gives Equation 29 till 31:

$$k_d=\frac{1.75\omega_n-B-k_\phi^2}{k_\phi} \tag{29}$$

$$k_p=2.15\omega_n^2\times JR \tag{30}$$

$$k_i=JR{\omega_n}^3 \tag{31}$$

Based on the Equation 32 and 33, damping ratio and damping frequency are calculated based on desired settling time and overshoot percentage of the system.

$$\omega_n=\frac{4}{\varsigma Ts} \tag{32}$$

$$\varsigma=OS\frac{\ln(/100)}{\sqrt{\pi^2+\ln^2(os/100)}} \tag{33}$$

where: ω_n = damping frequency
T_s = settling time
ζ = damping ratio
OS = percent overshoot

F. Prototype specification

The prototype consists of 24V DC brushless fan as a generator for a wind turbine. The DC fan was installed with hall sensor to allow non-contact measurement without impact the performance of wind turbine power generation. Figure 6 is prototype model that will be used during testing. The wind turbine uses parallel configuration to support more current into the system. Besides that, it has a single frame support structure for both wind turbines which can be controlled by the yaw actuator on the same time. The main braking system consists of dynamic braking with supported yaw angle control for horizontal furling operation.

Figure 6: Micro wind turbine system prototype

G. Drives circuit for yaw control and dynamic resistor

The H-drive drives circuit shown in Figure 7 widely used for motor control due to its flexibility of adjusting power and allow bi-direction of rotation in a DC motor. This can be accomplished by using pulse width modulation (PWM). The operation of H-bridge is shown in Table 2.

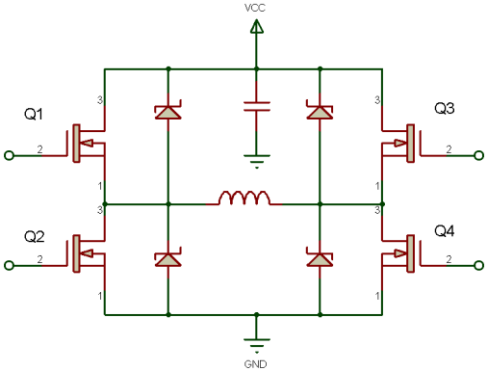

Figure 7: H bridge drives

Table 2
Operation of H-bridge

MOSFET				Description
Q1	Q2	Q3	Q4	
0	0	0	0	Motor stop
1	0	0	1	Motor turn clockwise
0	1	1	0	Motor turn counter clockwise
1	1	0	0	Short circuit
0	0	1	1	Short circuit

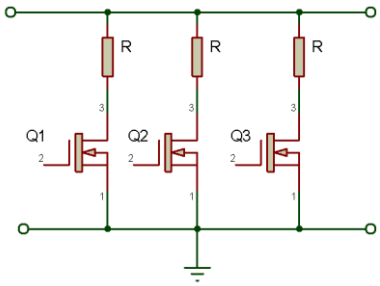

Figure 8: Dynamic braking resistor

Figure 8 shows dynamic braking resistor or dump load used to short-circuit the wind turbine when it draws a large current. PWM method is used to adjust the output voltage across the resistor. This is to ensure the rotor speed can be reduced to safety level by sink current into resistance. The formula to calculate duty cycle is in Equation 34.

$$V_{out} = D \times V_{in} \tag{34}$$

where: D = duty cycle
V_{out} = output voltage across resistor
V_{in} = input voltage

IV. Experimental Results

A. Hardware setup

Figure 9 represents an architecture of micro wind turbine system that consists several elements such as feedback element, controller, and energy harvester.

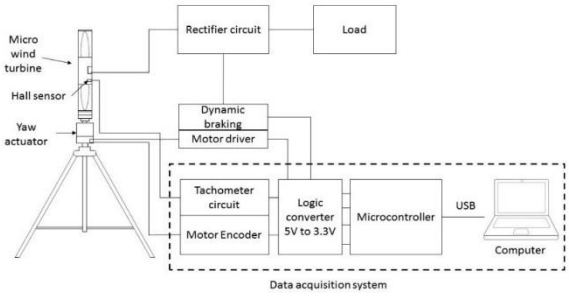

Figure 9: Architecture of controller system

The feedback element in this system is non-contact tachometer and motor encoder. Non-contact tachometer feeds information about the rotational speed of rotor into the controller. Meanwhile, motor encoder gives angle position which needed for yaw angle control. For the motor driver, it consists MOSFET which acts as a switch which allows bi-direction for DC motor. Dynamic braking system consists resistor that short circuit the generator winding. The energy harvester of the system is two module of micro wind turbine that converts wind power to electrical power. The microcontroller uses PID algorithm to control dynamic braking for speed regulation and a yaw control for over speed protection system. The data from the microcontroller was sent to the computer via USB interface. Parallax DAQ software is used during testing for data logging and analysis. Figure 10 and 11 is hardware that uses for testing purpose.

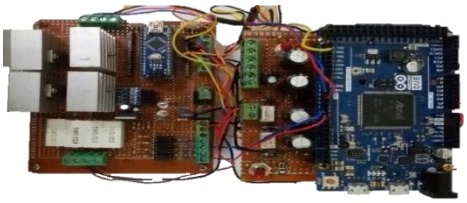

Figure 10: Controller braking system

Figure 11: Micro wind turbine during experiment

B. The Analysis of the prototype performance

The Figure 12 shows that the normal rotational speed operation for multi-rotor micro wind turbine without braking applied. The wind turbine configured by using the parallel connection. Since both wind turbines operated in parallel, the load is shared by using the single link. The average wind speed is in a range of 3.4 to 4.5 m/s during the measurement taken. The reason variation in average wind speed is due to the turbulence in wind and external source of wind blow which can be described as non-linearity that affect wind turbine. Where the waveform of rotational speed for both wind turbine is not stable. In worst case scenario, one of the wind turbines may experience difference effective wind speed as wind speed increased. This makes wind turbine operated exceed a maximum rotational speed that allowed. To handle this situation, dynamic braking system was used to slow down the rotational speed to a safe level.

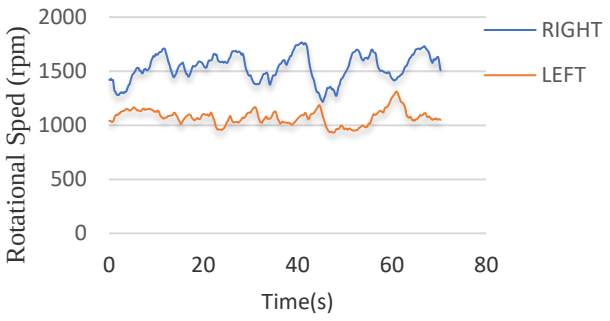

Figure 12: Rotational speed measurement for right and left position of micro wind turbine

C. Analysis of performance of dynamic braking system

Figure 13 shows the performance of dynamic braking during applied 30% and 63% PWM duty cycle where brake command was issued at 39.41 seconds for 63% braking, meanwhile, 30% braking applied was issued at 40.13 seconds which has slightly delay. The reason for long duration taken during measurement to ensure the system reached stable condition before brake command was issued.

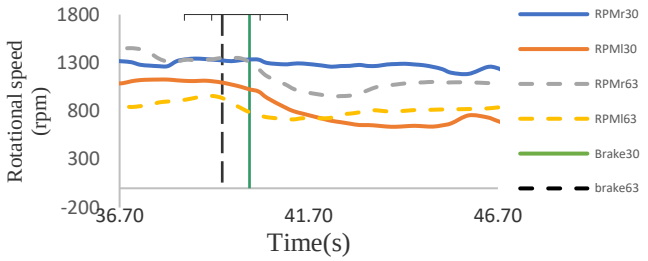

Figure 13: Transient respond of system

For 63% braking applied the highest rotational speed which in the right wind turbine shows the deceleration from 1353 to 952 rpm at 42.30 seconds before braking torque becomes too low to overcome aerodynamic torque. Meanwhile, for left wind turbine decelerate from 953 till 724 rpm at 42.06 seconds. For 30% braking applied, it shows very slow deceleration for a right wind turbine from 1334 till 1186 rpm at 45.93 seconds. In meanwhile, the left wind turbine decelerates from 1025 till 639 rpm at 43.77 seconds. The result was summarized in Table 3 and 4 for comparison between 63% and 30% braking. The result from Table 3 and 4 show that the system does not have settling time because it does not have steady state condition. Comparison performance between 30% and 63% braking, shows that the higher braking setting can slow wind turbine much faster compared to a lower braking setting.

Table 3
Dynamic braking for 63%

Position of micro wind turbine	Initial rotational speed(rpm)	Final rotational speed(rpm)	Time to reach(s)
Right	1352	952	2.89
Left	953	724	2.65

Table 4
Dynamic braking for 30%

Position of micro wind turbine	Initial rotational speed(rpm)	Final rotational speed(rpm)	Time to reach(s)
Right	1334	1186	6.52
Left	1025	639	4.36

Figure 14 shows the various deviation in yaw angle with a respect to the rotational speed. Deviation in yaw angle will reduce the aerodynamic torque entered on the wind turbine blade. As the yaw angle approach to 90 degrees, the wind turbine has lower rotational speed. This can be seen in yaw angle of 75 degrees which have lowest rotational speed about 224 rpm compared to the 15-degree of yaw angle which is 1303 rpm. For 90 degree of yaw angle will cause wind turbine stop operating since this micro wind turbine has its own casing, it protects from wind flow into the blade that causes the rotor to turn.

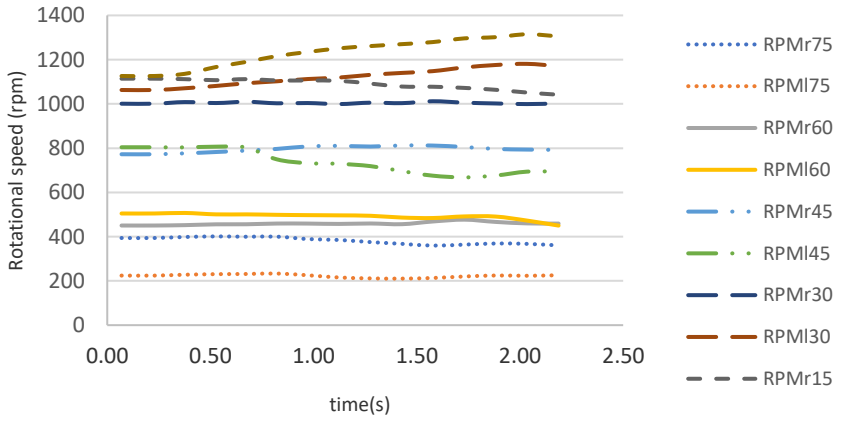

Figure 14: Yawed wind turbine

D. ITAE tuning

The design objective for dynamic braking system is to keep the micro-wind turbine speed within set point which is 1200 RPM. The design parameter of the system is 10% overshoot, damping factor is 0.59 and settling time is 100 seconds. A longer settling time is used to gain lower integral coefficient. As a result, the effect of integral term in reducing steady state error is decreased. In contrary, high value of integral term tends to make pattern output become oscillate around the set point. Meanwhile, for yaw control design, the criteria are 5% overshoot with damping ratio 1.932 and the settling time is 3 seconds. Fast setting time for yaw control design is used for fast response when the speed reaches trigger value of 1300 RPM. This to ensure the wind turbine from over speed that caused by increasing wind speeds. The PID coefficient can be computed for dynamic braking using equation 24 till 26 which resulting in Table 5.

Table 5
Controller gain

Proportional gain, k_d	Integral gain, k_p	Derivatives gain, k_i
31.38	2.53	0.1065

From the ITAE tuning for dynamic braking, it shows the differential gain is high compare others. This initial value will be reduced to avoid excessive action from differential term by manual tuning. By using equation 29 till 31, PID coefficient calculated as in Table 6:

Table 6
Controller gain

Proportional gain, k_d	Integral gain, k_p	Derivatives gain, k_i
3.3	0.102	0.092

The final manual tuning by using PID control for dynamic braking is in Table 7.

Table 7
Controller gain

Proportional gain, k_d	Integral gain, k_p	Derivatives gain, k_i
0.137	0.005	0.1316

E. Over speed protection and speed regulation

Figure 15 shows the response of the system when wind speed increase from to 3.9 to 6 m/s. The wind turbine speed was set to 1200 rpm for safe operations speed. Meanwhile, the maximum speed was set to 1300 rpm for over speed protection test. Initially, dynamic braking start operates regulate speed around 1200 rpm. When wind speed increased, where the dynamic braking cannot cope with the increment of rotational speed, yaw control start takes over the control. When yaw angle start elevates to 30 degrees, the speed was reduced from 1308 rpm to 1142 rpm at the time taken is 4.68seconds. The result was summarized in Table 8.

Table 8
Overspeed testing

Initial rotor speed (Rpm)	Final rotor speed(Rpm)	Time was taken(s)
1308	1142	4.68

From Table 8, time is taken to slow down rotor speed which around 4.68 second this due to delay in mechanical action. As result, the timing for settling time for yaw actuator that previously tuning with ITAE was increased.

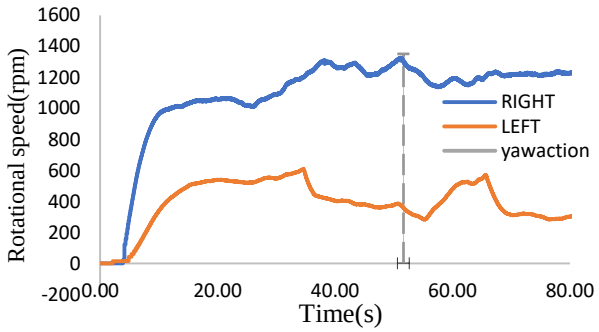

Figure 15: Overspeed test

F. Comparison between yaw braking and cascade braking system

The test is conducted to compare the performance of braking mechanism to maintain the rotational speed from over speed. The over speed value is set at 1300 rpm in the experiment. Figure 17 is wind turbine braking speed pattern by using yaw control. These over speed conditions start when wind speed increased from 4.5 to 4.8 m/s. without dynamic braking control, the wind turbine cannot sustain the rotational speed from reaching over speed limit. The yaw angle was changed from 0 to 60 degree to slow the wind turbine speed with the time taken is 6.79 seconds. Implementation cascade braking in Figure 18 by using dynamic braking and yaw control. It shows that the rotational speed can be maintained without reaching over speed condition with average time taken is 0.3 seconds. The wind turbine can maintain a rotational speed below over speed limit when wind speed increase from 4.5-5.2 m/s while the yaw angle at the moment, increased from 0 to 45 degrees.

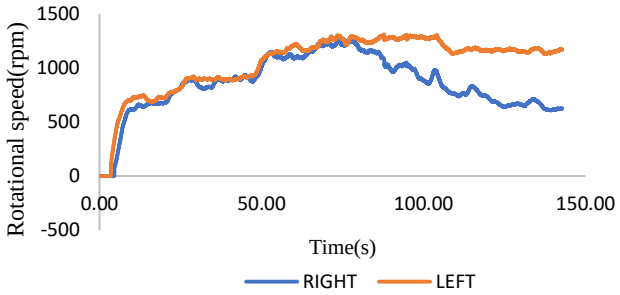

Figure 17: Over speeding protection by using yaw braking

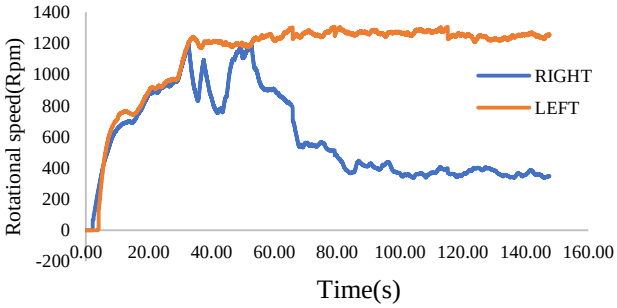

Figure 18: Speed regulation with over speed protection

The test is conducted to compare the performance of braking mechanism to maintain the rotational speed from over speed. The over speed value is set 1300 rpm in the experiment. Figure 17 is wind turbine braking by using yaw control. These over speed conditions start when wind speed increased from 4.5 to 4.8 m/s. without dynamic braking control, the wind turbine cannot sustain the rotational speed from reaching over speed limit. The yaw angle was changed from 0 to 60 degree to slow the wind turbine speed with the time taken is 6.79 seconds. Implementation cascade braking in Figure 18 by using dynamic braking and yaw control. It shows that the rotational speed can be maintained without reaching over speed condition with average time taken is 0.3 seconds. The wind turbine can maintain a rotational speed below over speed limit when wind speed increase from 4.5-5.2 m/s while the yaw angle at the moment, increased from 0 to 45 degree.

G. Analysis of braking system in full stop operation

Figure 19 shows the transient response of wind turbine when stop command was issued when maximum speed is reached. During this condition, yaw actuator operates with dynamic braking for full stop operation. For yaw actuator, the angle was adjusted to 90 degrees to block incoming wind from enters wind turbine. Meanwhile, dynamic braking was operating at full setting to ensure faster stopping time. Time taken for rotational speed reduced to 0 rpm is 4.4 seconds when controller gives the command at 13.68 seconds.

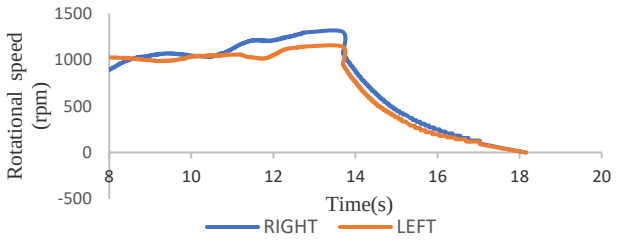

Figure 19: Stop condition wind turbine

V. DISCUSSIONS

The yaw controls for braking application involving with manipulation in aerodynamic torque. The advantage of involving aerodynamic is that it is able to stop the micro wind turbine operation by making it out of alignment toward wind direction. The disadvantage of this system braking response is slower due to delay in mechanical actuator which is 6.79 seconds. Meanwhile, for the dynamic braking system, it is an electrical braking mechanism by short circuit the winding. Therefore, it can achieve a faster response in braking, which is 0.04 seconds. However, braking power based on the power generated by a wind turbine. Thus, it only able to slow down the rotational speed and not a suitable for shutdown operation application.

Cascade braking system involving with dynamic braking and yaw control. From the experiment, it shows that the braking system able to maintain the rotational speed under maximum speed when wind speed increased. Compared with the yaw control system alone, increasing yaw angle result loss in power generated if high wind speed just momentarily. The weakness in this system is similar to yaw control system because of additional delay in yaw actuator. The performance of speed regulation mainly depends on the dynamic braking system since the yaw control and dynamic braking working separately in this project.

VI. CONCLUSION

Implementation of dynamic braking system shows the faster time response which is 0.04 seconds compare with yaw control. Meanwhile, in yaw control for the braking application, the time response is 6.79 seconds. The cascade braking mechanism base on dynamic braking and yaw control yields time response of 0.3 seconds to overcome the limitation in dynamic braking and yaw control. The speed regulation performance depends on wind speed because generator torque produced by dynamic braking was limited and inconsistent due to power generated required to brake. The changes in rotational speed as feedback for the controller to prevent micro wind turbine from the over speed. Since the aerodynamic torque considers as unmeasured parameter or disturbance into the system, less sensor is required.

ACKNOWLEDGMENT

The author would like to credit University Malaysia Perlis for providing aid through project supervision and permission to use Center of Excellent for Fenewable Energy (CERE), School of Electrical System Engineering facilities and equipment.

REFERENCES

[1] M. T. Velázquez, M. Vega, D. Carmen, J. A. Francis, L. a M. Pacheco, and G. T. Eslava, “Design and Experimentation of a 1 MW Horizontal Axis Wind Turbine,” vol. 2014, no. January, pp. 9–16, 2014.

[2] L. Ledo, P. B. Kosasih, and P. Cooper, “Roof mounting site analysis for micro-wind turbines,” Renew. Energy, vol. 36, no. 5, pp. 1379–1391, 2011.

[3] Z. Li and A. Reynolds, “Domestic Application of Micro Wind Turbines in Ireland : Investigation of Their Economic Viability economic viability,” pp. 0–11, 2011.

[4] Z. Wu and H. Wang, “Research on Active Yaw Mechanism of Small Wind Turbines,” Energy Procedia, vol. 16, pp. 53–57, 2012.

[5] C. P. Butterfield, E. Muljadi, and T. Forsyth, “Soft-Stall Control Control for Small wind turbine power regulation,” Colorado, 1998.

[6] N. Mcmahon, “On Electrodynamic Braking for Small Wind Turbines Generator Geometry and Its Effect on Short- Circuit Torque,” no. November 2012, pp. 2012–2013, 2013.

[7] S. Saini, “Review of Doubly Fed Induction Generator Used in Wind Power Generation,” vol. 4, no. 2231, pp. 53–56, 2013

[8] a Mesemanolis and C. Mademlis, “Combined Maximum Power Point and Yaw Control Strategy for a Horizontal Axis Wind Turbine,” pp. 1–7, 2014.

[9] Y. She and X. She, “Plug-and-play control module for variable speed wind turbine under unknown aerodynamics,” IECON Proc. (Industrial Electron. Conf., pp. 205–210, 2010.

[10] C. Evangelista, P. Puleston, F. Valenciaga, and L. Fridman, “Lyapunov Designed Super-Twisting Sliding Mode Control for Wind Energy Conversion Optimization,” no. c, pp. 1–8, 2011.

[11] H. Choi, J. Kim, J. Cho, and Y. Nam, “Active Yaw Control of MW class Wind Turbine,” Int. Conf. Control. Autom. Syst., pp. 1075–1078, 2010.